Articles

Amine−Guanidine Switch: A Promising Approach to Improve DNA Binding and Antiproliferative Activities

Keiichiro Ohara,[†] Michael Smietana,*[,†] Audrey Restouin,[‡,§,||] Séverine Mollard,[‡,§,||] Jean-Paul Borg,[†,§,||] Yves Collette,*[,‡,§,||] and Jean-Jacques Vasseur[†]

Institut des Biomolécules Max Mousseron, UMR 5247 CNRS−UM I−UM II, Université de Montpellier II, CC008, Place E. Bataillon, 34095 Montpellier Cedex 5, France, INSERM U599, Centre de Recherche en Cancérologie de Marseille, TrGET platform, 13009 Marseille, France, Institut Paoli-Calmettes, 13009 Marseille, France, and Université de la Méditerranée, 13007 Marseille, France

Received September 25, 2007

A series of polyaromatic guanidino derivatives was synthesized and evaluated for growth inhibitory properties in several human carcinoma cell lines. The properties of these guanidino compounds were compared to those of their corresponding synthetic amino precursors. The size of the polyaromatic ring system as well as the length of the tether attached to the ring had a direct impact on the observed antiproliferative profiles, compound **14** having the broadest spectrum of activity. As both series intercalate DNA, guanidine derivatives showed a remarkable affinity for DNA and the guanidinium group appeared to be essential, yet not sufficient for caspase-3/7 activation. Compound **14** also showed significant in vivo activity against breast cancer cell xenografts in NOG/SCID mice. These results suggest that the electronic nature of chain tethering an intercalator not only influences the DNA-binding process but also controls the antitumoral activity of the whole compound.

Introduction

DNA is one of the most challenging bioreceptor for small molecules and a target of choice for the control of gene expression.[1] In this context, DNA-binding molecules constitute an important class of drugs in anticancer therapy.[2] Although it is well-established that DNA binding is not sufficient to confer cytotoxic activities, interaction with DNA is often considered as a necessary criteria to maintain a cytotoxic effect. Groove binders and intercalators are the two principal categories of DNA-binding drugs.[2] The later represents an important class of antitumoral DNA binders and is characterized by the insertion of planar aromatic or heteroaromatic rings in between DNA base pairs.[3,4] Pertinent examples include the anthracyclines, acridines, and ellipticines[5,6] which are thought to poison topoisomerases I and II.[7] Several factors including hydrogen bonding and π-stacking play a role in the stabilization of the drug–DNA complex, and polycyclic aromatic hydrocarbons (PAHs)[a] constitute an important family for the design of new chemotherapeutic DNA intercalators.[8,9] In particular, antitumor activity was discovered in PAHs bearing either the anthracene[9−12] or the pyrene ring systems.[13−16]

Recently, we used MALDI-TOF mass spectrometry to observe complexes between single-stranded oligonucleotides and various structurally distinct guanidinium derivatives. This study revealed the importance of the guanidinium group and emphasized the importance of the presence of an aromatic ring for a better interaction.[17] In light of the importance of the guanidinium group in antimicrobial,[18] antitrypanosomal,[19] and, above all, antitumoral agents,[20,21] we decided to undertake a study to evaluate the correlation between the ability of these compounds to bind to DNA and their resultant cytotoxic activity. We anticipated that such molecules would intercalate DNA and generate a complementary guanidinium−phosphate interaction which would contribute to the formation of stable complexes. The specific patterns of hydrogen bonding and the high basicity of the guanidinium groups may confer to these compounds biochemical and biophysical attributes well-amplified with respect to their parent amines. To test this hypothesis and evaluate the importance of the guanidinium function, we examined a series of aromatic and polyaromatic guanidinium derivatives and compared their behavior with their corresponding amino counterparts (Figure 1). In this paper, we report their synthesis, biological activities, and DNA-binding properties.

Chemistry. Conjugates **1**−**16** were synthesized in order to probe how variations of the substituted guanidine function influenced the cytotoxicity (Figure 1). For example, **2**, **4**, **6**, **8**, and **10** were synthesized to probe the influence of the aromatic or polyaromatic moiety, while **10**, **14**, **15**, and **16** were prepared to describe the nuances surrounding the tether. Moreover, their amino precursors were selected to enable direct comparison and immediate identification of functional requirements.

As shown in Scheme 1, the syntheses of target guanidines **2**, **4**, **6**, **8**, and **10** require the corresponding amino compounds as precursors. These amines were commercially available (**1**, **3**, and **9**) or generated from the corresponding aldehydes. Hence,

* To whom correspondence should be addressed. Phone: 33 4 67 14 38 37. Fax: 33 4 67 04 20 29. E-mail: msmietana@univ-montp2.fr (M.S.). Phone: 33 4 91 75 84 13. Fax: 33 4 91 26 03 64. E-mail: collette@marseille.inserm.fr (Y.C.).

[†] IBMM, Université Montpellier II.

[‡] INSERM U599.

[§] Institut Paoli Calmettes.

[||] Université de la Méditerranée.

[a] Abbreviations: PAH, polycyclic aromatic hydrocarbon; MALDI-TOF, matrix-assisted laser desorption ionization time of flight; CT-DNA, calf-thymus DNA; bp, base pair; BOC, *t*-butyl-oxycarbonyl; T_m, melting temperature; BPE, bisphosphate buffer ethylene diamine tetracetic acid; DMSO, dimethylsulfoxide; DIEA, diisopropylethylamine; PBS, phosphate-buffered saline; NOG/SCID, nonobese gamma/severe combined immunodeficiency mice.

10.1021/jm701207m CCC: $37.00
Published on Web 12/04/2007

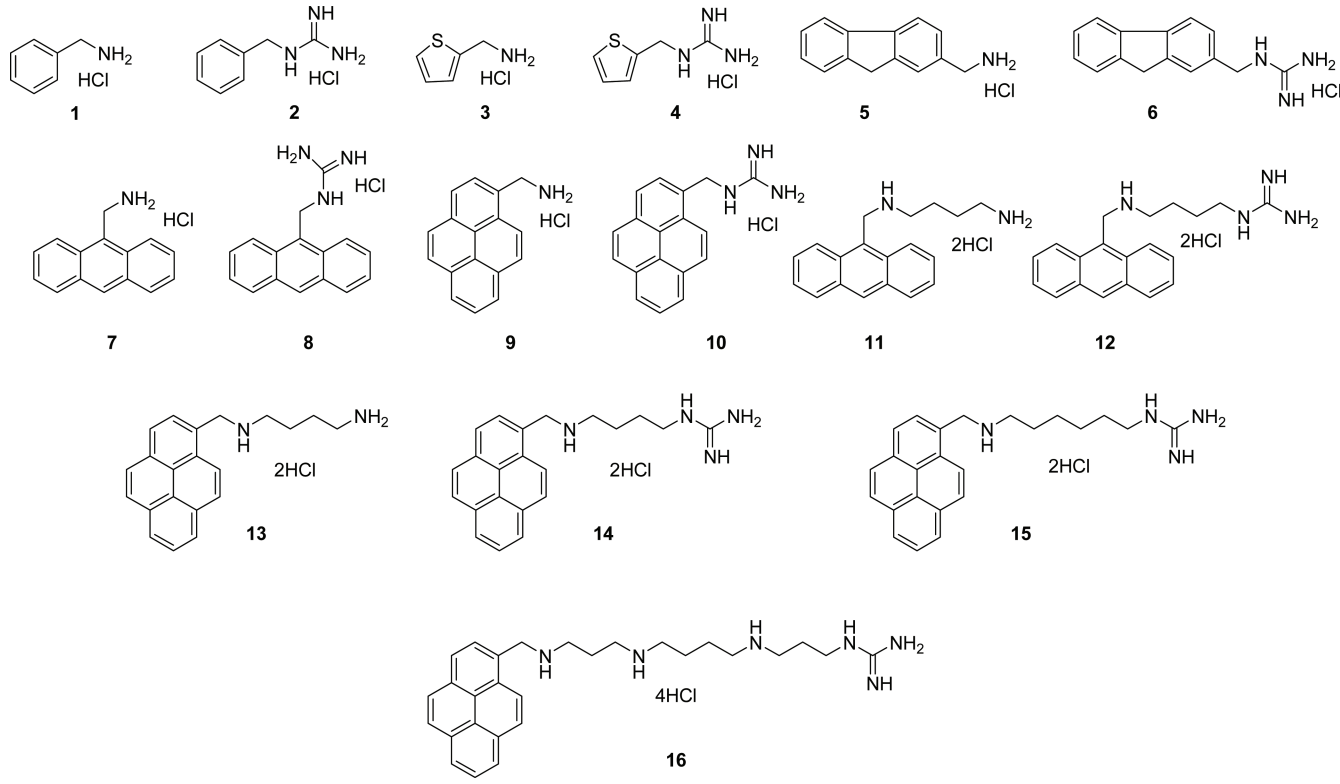

Figure 1. Structures of compounds **1**−**16**.

Scheme 1[a]

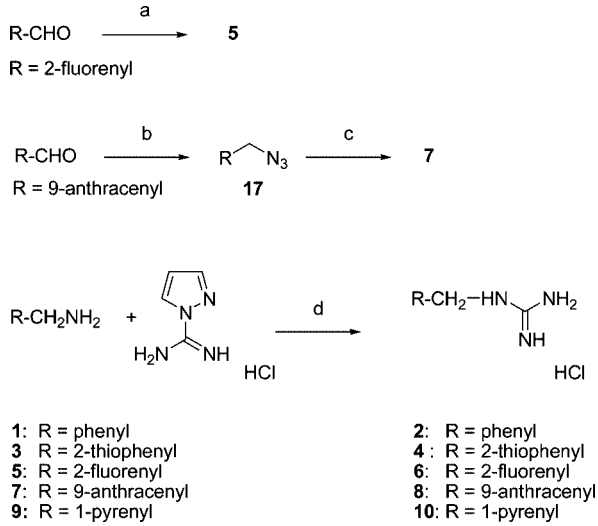

[a] Reagents: (a) (i) $NH_2OH \cdot HCl$, AcONa, H_2O, EtOH, reflux; (ii) H_2, Pd/C, MeOH, EtOAc; (iii) HCl gaz, MeOH; (b) (i) $NaBH_4$, $CHCl_3$, MeOH, 0 °C to rt; (ii) $SOCl_2$, CH_2Cl_2, 0 °C; (iii) NaN_3, DMF, 50 °C; (c) (i) H_2, Pd/C, MeOH, EtOAc; (ii) HCl gaz, MeOH; (d) DIEA, DMF.

synthesis of 2-fluorenemethylamine **5** began with oximation of commercially available fluorenecarboxaldehyde, followed by reduction with hydrogen over palladium on activated carbon (H_2, Pd/C). In the case of 9-anthracenemethylamine **7**, stability issues led us to reduce the aldehyde function with $NaBH_4$ and perform the synthesis starting the synthesis with the corresponding alcohol,[22] which was converted via chlorination followed by nucleophilic substitution with sodium azide to the corresponding azido derivative **17**. The reduction procedure described above (H_2, Pd/C) was used to convert **17** to the corresponding free amine. These amines were further precipitated by HCl bubbling in MeOH to form the target HCl salts **5** and **7**. With

Scheme 2[a]

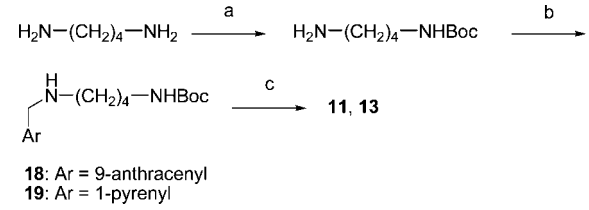

[a] Reagents: (a)Boc_2O, CH_2Cl_2, 0 °C; (b) (i) ArCHO, MeOH/THF; (ii) $NaBH_4$, MeOH/THF, 0 °C to rt; (c) HCl gaz, MeOH.

these amine salts in hand the guanidino analogues were prepared by direct guanidylation using 1*H*-pyrazole-1-carboxamidine hydrochloride as the guanidylating reagent thus giving guanidines **2**, **4**, **6**, **8**, and **10** in good yields.[23]

The synthesis of amines **11** and **13** (Scheme 2) began by *N*-Boc protection of commercially available 1,4-butanediamine[24] followed by reductive amination with the corresponding aldehyde to give intermediates **18** and **19**, respectively. These compounds were converted to the desired amines **11** and **13** by HCl bubbling in methanol.

Finally, polyaromatic-branched guanidino derivatives **12**, **14**, **15**, and **16** were prepared in a three-step process which involves the reaction of either butyl- or hexyldiamine with diBoc-thiourea followed by reductive amination with the corresponding aldehyde (Scheme 3). In the case of spermine, purification problems were encountered with diBoc-protected intermediate **26** and all secondary amine functions were further protected with Boc_2O to give the resultant derivative **27**. Deprotection of all Boc-protecting groups in **23**−**25** and **27** was subsequently accomplished by HCl bubbling in MeOH thus providing the guanidines **12**, **14**, **15**, and **16** in good overall yields.

DNA-Binding Properties. Melting temperatures were measured for the compounds bound to calf-thymus (CT) DNA (42% GC bp) to obtain a qualitative evaluation of the DNA-binding

Scheme 3[a]

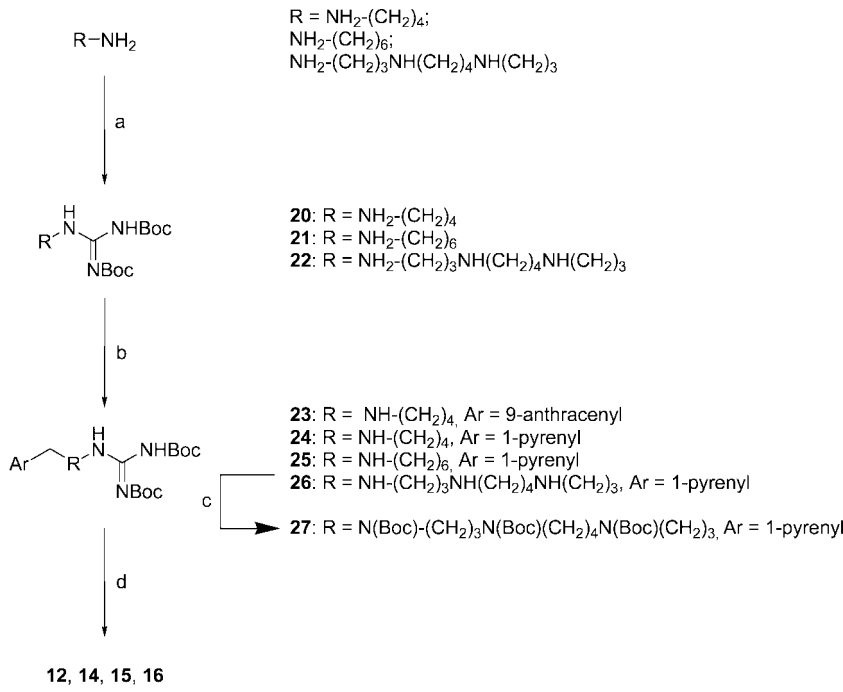

[a] Reagents: (a) *N*,*N*′-diBoc-thiourea, DMF; (b) (i) ArCHO, MeOH/THF; (ii) $NaBH_4$, MeOH/THF, 0 °C to rt; (c) Boc_2O, CH_2Cl_2; (d) HCl gaz, MeOH.

Table 1. Double-Stranded DNA Thermal Stability in the Presence of Compounds **1**–**16**[a]

compd	ΔT_m CT-DNA NaCl 0 M[b]	ΔT_m oligo NaCl 0 M[c]	ΔT_m oligo NaCl 0.1 M[d]	compd	ΔT_m CT-DNA NaCl 0 M[b]	ΔT_m oligo NaCl 0 M[c]	ΔT_m oligo, NaCl 0.1 M[d]
1	0	0.1	0	**10**	8.1	19.0	6.0
2	0.1	0.1	0	**11**	13.1	26.0	8.0
3	0.1	0	0	**12**	15.1	28.1	9.0
4	0.1	0	0	**13**	20.2	32.1	10.0
5	1.0	0.1	0	**14**	nd[e]	34.2	12.0
6	0	1.0	0	**15**	nd[e]	34.1	12.0
7	3.0	9.0	1.0	**16**	nd[e]	39.1	16.0
8	6.1	15.0	4.0	**EtBr**	8.1	21.0	5.0
9	5.0	15.0	3.0	**Hoechst 33258**	9.0	25.1	12.0

[a] T_m measurements were performed at 260 nm with a heating rate of 0.5 °C/min. [b] In BPE buffer, pH 7.0 (6 mM Na_2HPO_4, 2 mM NaH_2PO_4, 1 mM EDTA) using 2 μM drug and 4 μM bp CT-DNA (T_m = 69.0 °C without any drug). [c] In cacodylate buffer, pH 7.0 (9.8 mM) using 12 μM drug and 2 μM oligo d(ACACCCAATTCT) and 2 μM of its complementary sequence d(AGAATTGGGTGT) (T_m = 29.0 °C without any drug). [d] In cacodylate buffer, pH 7.0 (9.8 mM, NaCl 100 mM) using 12 μM drug and 2 μM oligo d(ACACCCAATTCT) and 2 μM of its complementary sequence d(AGAATTGGGTGT) (T_m = 46.0 °C without any drug). [e] Not detectable (T_m > 100 °C).

affinity of these drug candidates (Table 1). Since several of the compounds bound very strongly to CT-DNA, the interaction of the compounds with a shorter dodecamer duplex d(ACACCCAATTCT)/d(AGAATTGGGTGT) (42% of GC bp) was also studied (Table 1). The reduced binding of the drugs to the dodecamer duplex, reflected by the lower T_m values of the drug−dodecamers complexes, allowed for a better relative comparison for the DNA-binding affinity of the putative intercalating agents. Determination of the melting temperature was thus performed in the absence of any salt addition in both experiments. Whereas the ΔT_m values with the dodecamer were measured with 6 equiv of each compound in sodium cacodylate buffer (9.8 mM, pH 7.0), we were unable to obtain an accurate ΔT_m for most of the complexes formed with CT-DNA at a drug/CT-DNA ratio of 0.5, because a plateau in the melting curve was not obtained before 100 °C. However, by changing the buffer to BPE (6 mM Na_2HPO_4, 2 mM NaH_2PO_4, 1 mM EDTA, pH 7) and lowering the CT-DNA concentration to 4 μM bp, accurate values of ΔT_m were obtained for most of the candidates (except **14**, **15**, and **16** for which a plateau could not be observed before 100 °C). Inspection of Table 1 shows that hydrogen bonding abilities and ionic interactions of amino and guanidino functions are not sufficient to induce the formation of a stable drug/DNA complex and neither amines **1**, **3**, and **5** nor guanidines **2**, **4**, and **6** seem to stabilize DNA. However, hydrophobicity brought by polyaromatic ring systems appears to be particulary relevant to the complexes formed with DNA. Indeed, whatever their substituent, anthracene and pyrene ring systems induce notable stabilization of the drug/DNA complex. Moreover, for a specified terminal amino- or guanidinotether, the pyrene was found to induce a greater stabilization than the anthracene ring system. The same pattern was found in more physiological conditions (NaCl 100 mM), although, as expected, the ΔT_m values were lowered (Table 1). These results confirm the reduced contribution of the hydrogen bond in aqueous media due to entropic effects and solvatation, whereas hydrophobic forces and $\pi-\pi$ interactions naturally become stronger. Nevertheless, a good correlation of the duplex stabilization is found with the net charge of the compounds, anthracenyl-based diamine **11** inducing a greater stabilization than pyrenyl-based guanidine **10** and compound **16** inducing the strongest ΔT_m with the dodecamer duplex whereas a plateau could not be reach with CT-DNA. As expected, for a given structure, ΔT_m values for both CT-DNA and the dodecamer, the "Y-shaped" guani-

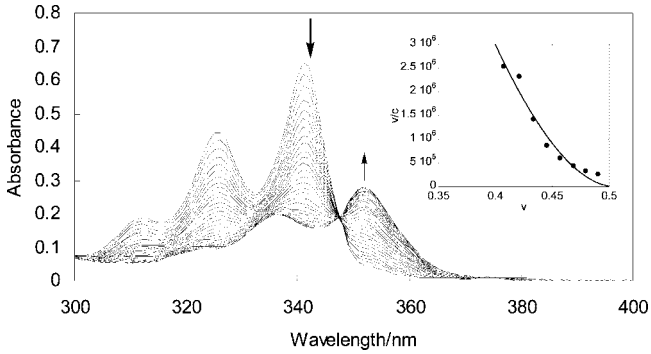

Figure 2. Absorption titration of compound **14** (20 μM) in sodium cacodylate buffer (9.8 mM) with pH 7.0 and increasing concentration of CT-DNA (from top to bottom 0–50 μM bp). (inset) Scatchard plot for the binding of **14** to CT-DNA. Values for binding ratio υ and free compound concentration c were determined from data taken from the spectrophotometric titration.

Table 2. DNA Binding Properties

compd	RS[a] (nm)	H[b] (%)	$K \times 10^5$ M^{-1}	n[c]	R[d]
7	8	64	1.30	1.9	0.98
8	7	70	8.68	1.9	0.97
9	11	70	6.46	1.8	0.95
10	10	73	14.54	1.9	0.97
13	11	74	111.11	2.0	0.96
14	11	75	408.11	2.0	0.98
15	11	75	361.56	1.9	0.97
16	11	85	228.18	2.0	0.99
EtBr	39	56	25.80	1.8	0.98

[a] Red shift observed between the wavelengths of maximum absorption for free and DNA-bound compounds. [b] Hypochromicity ($H = 1 - \varepsilon_{bound}/\varepsilon_{free} \times 100$), where ε_{free} and ε_{bound} are the extinction coefficients for free and DNA-bound compounds. [c] Number of base pairs per binding site. [d] Correlation coefficient.

dinium function, appear to induce a stronger stabilization than the ammonium one. This can be explained by the hydrogen bonding ability of the guanidine function as well as its higher pK_a (pK_a > 11) which is fully protonated at pH 7 as compared to the primary amine (pK_a = 8–10), thus contributing more significantly to the binding by ionic interactions with the negatively charged phosphates of DNA. Finally, compounds **11**−**16** were found to induce a greater stabilization than the well-known DNA binders ethidium bromide and Hoechst 33258, which were evaluated under the same conditions.

Mechanism of Action Studies. Anthracenemethylamine **7** and pyrenemethylamine **9** have already been shown to intercalate with DNA,[15,25] and UV–visible titration spectra obtained with our guanidinium derivatives are similar to those generally reported for other pyrene- or anthracene-based compounds in the presence of DNA.[26–28] Figure 2 provides an example illustrating the characteristic changes in the absorption spectra during titration of **14** with increasing amounts of CT-DNA. The binding of the drug was characterized by a strong hypochromicity (75%), an 11 nm red shift (from 341 to 352 nm), and the formation of a well-defined isosbestic point at 347 nm. Similar profiles were observed for all investigated guanidinium derivatives (Table 2) which suggest the intercalation of the drug between DNA base pairs. The spectral changes observed in the absorption titrations of these compounds with CT-DNA were used to generate nonlinear Scatchard binding isotherms (Figure 2, inset) using the noncooperative site exclusion model of McGhee−Von Hippel.[29] The binding parameters (K, n) obtained are shown in Table 2 with K being the apparent binding constant and n the number of base pairs per bound molecule. All derivatives studied interact strongly with native DNA, reflecting ΔT_m values analysis: (1) the guanidinium function induces a stronger binding than the related ammonium (compare compounds **7–14**); (2) the pyrene ring system binds more strongly than the anthracene ring system (compare **8** and **10**). These results indicate the importance of the guanidinium function on the binding, presumably due to its greater stability as an ion in an aqueous environment. However, the net charge of the compounds appears to have a major effect on the binding for structurally close molecules (compare **10** and **13**), whereas increasing electrostatic interactions on a given guanidinium molecule by adding positively charged nitrogen moderate the DNA-binding strength (compare **14** and **16**). It should be noted that, in the case of **16**, a significant change in the absorbance spectra at high DNA concentration was observed, suggesting a second mode of binding. In fact, a strong hypochromism (85%) and a substantial red shift (11 nm) was observed with DNA concentration increasing from 0 to 50 μM bp. But two new red-shifted electronic bands (at 336 and 352 nm) develop upon further addition of DNA, indicating a second distinct binding mode (data not shown). This increase in absorbance above 300 nm at high binding ratios is attributed to the interaction of the polyammonium tether with the phosphate groups of DNA as polyamines are known to bind to the double helix and cause condensation.[30,31] Nevertheless, derivatives **13–16** interact strongly with affinity constants around 10^6 M^{-1}, which is 10 times higher than the well-known intercalator ethidium bromide used here as a reference and measured under the exact same conditions. The number of base pairs per bound molecule obtained with these compounds were consistent with the intercalating mode where the planar polyaromatic ring system is stabilized by extensive van der Waals interactions with the bases of the DNA helix.

In order to attest unambiguously the behavior of these polyaromatic guanidines, DNA viscosity measurements were conducted. Intercalation of planar aromatic rings into DNA is accompanied by an effective increase of the DNA contour length, L/L_0, as well as the viscosity of the DNA polymer. Therefore, viscometric titrations represent a highly reliable method for establishing the binding modes of DNA interacting ligands.[32] The viscometry data are usually presented as plots of L/L_0 versus r (molar ratio of added compound to DNA base pairs) yielding the slopes m which fall between 0.5 and 1.5 for monofunctional intercalators such as ethidium bromide, while classical groove binder such as Hoechst 33258 produces a slope of zero.[33,34] In our case, when L/L_0 is plotted versus r, the least-squares fitting for all guanidines tested gives slopes which all fall within the range expected for monfunctional intercalators (m = 1.20, 0.91, 0.75, 0.86, and 0.82 for guanidines **8**, **10**, **12**, **14**, and **16**, respectively, Figure 3). As controls, the slopes of ethidium bromide and Hoechst 33258 (1.02 and 0.08, respectiveley) were found to be near the predicted slope of 1.0 and 0. These results provide strong evidence that these guanidines associate with double stranded DNA via intercalation. Interestingly, even compound **16** appears to favor intercalation at low binding ratios.

Recently, the amines at the 3 and 8 positions of the well-known DNA intercalating agent ethidium bromide, were converted into guanidines.[35] The authors demonstrated that this double amine−guanidine substitution changed the original intercalator into a minor groove binder of DNA. Moreover, the new bis-guanidinium derivative was found to bind to DNA more tightly than the parent ammonium. This is in agreement with our study, which helps to go further, by demonstrating that a fine-tuning might be found with a single amine−guanidine

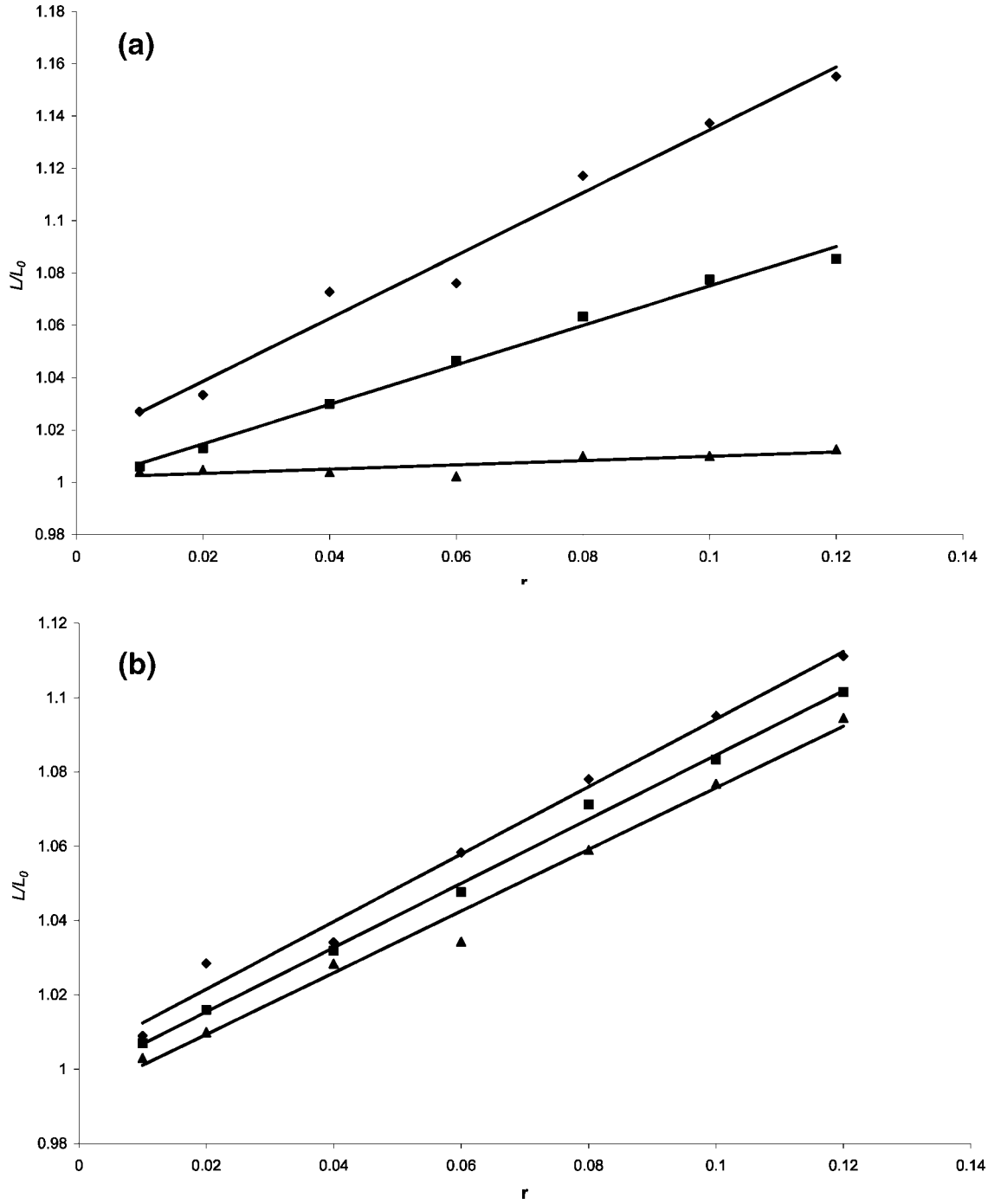

Figure 3. (a) Relative length increase (L/L_0) of anthracenyl derivatives **8** (♦ slope = 1.20) and **12** (■ slope = 0.75) and the groove binder Hoechst 33258 (▲ slope = 0.08). (b) Relative length increase (L/L_0) of pyrenyl derivatives **10** (♦ slope = 0.91), **14** (■ slope = 0.86), and **16** (▲ slope = 0.82). The contour lenghts in the presence (L) or absence (L_0) of the compounds were calculated from viscosity measurements on sonicated calf thymus DNA.

switch. In our case, a single amine−guanidine exchange in known intercalators[15,25] resulted in a marked gain of affinity while keeping their intercalative mode of binding.

Biology. In Vitro and In Vivo Antiproliferative Activity. The biological activity of these intercalators was first evaluated in the SKBR3 breast cancer cell line (Table 3). Although there is no direct relationship between DNA binding and antiproliferative activity, it was found that within a series of compounds, some guanidinium derivatives typically reduced cell proliferation and/or viability more potently than their ammonium precursor. Though these pairs should be nearly identical in their lipophilicity, the higher degree of ionization of the guanidinium group seems to increase the resultant antiproliferative activity. A strong stabilization of the target DNA as well as a better cellular uptake might explain these differences, and in the case of the SKBR3 cells, **14** was found to be the most active compound. To check whether the polyaromatic ring might significantly influence the antitumoral activity, these guanidino compounds were further tested for their potential antiproliferative effect on a panel of five other human cancer cell lines: BT474 (breast carcinoma); T47D (breast carcinoma); LnCAP (prostate carcinoma); PC-3 (prostate carcinoma); HT-29 (colon carcinoma). Most tested compounds displayed antiproliferative activity in the micromolar range

Table 3. In Vitro Antitumoral Activities for Various Ammonium and Guanidinium Derivatives

SKBR3				IC_{50}[a]				
ammonium derivatives	IC_{50}[a]	guanidinium derivatives	IC_{50}[a]	BT474	T47D	LnCAP	PC-3	HT-29
1	>40	**2**	>40	47.9	83.2	43.7	>100	>100
3	>40	**4**	>40	95.5	85.1	64.6	>100	>100
5	>40	**6**	15.7	19.1	6.9	27.5	24.0	32.4
7	25.5	**8**	1.9	19.1	29.5	3.5	10.0	>100
9	12	**10**	11.0	33.9	43.7	93.3	43.7	39.8
11	3.3	**12**	2.3	14.5	30.9	28.2	13.8	79.4
13	4.2	**14**	1.9	16.2	2.2	9.3	7.9	30.9
		15	4.8	29.2	2.2	nd[b]	nd[b]	nd[b]
		16	25.3	34.6	8.0	nd[b]	nd[b]	nd[b]

[a] Drug concentration (μM) required to inhibit cell growth by 50%. All assays were performed in triplicate. [b] Not determined.

(Table 3). As expected, the nature of the ring appears to play a major role in the activity. Whereas the phenyl or the thiophenyl rings seem to induce only a slight effect, the activity increases with the number of cycles in the aromatic moiety. The butylamino tether does not seem to influence the activity related to the anthracenyl ring (compare **8** and **12**) but definitely increases the potency of the pyrenyl ring (compare **10** and **14**), **14** having the broadest spectrum of activity. Moreover, the length of the alkyl chain in the tether seems to barely affect the activity, **15** having almost the same potency than **14** on every cell line tested. However, a strong stabilization of the DNA duplex structure, reflected by a strong binding constant as with **16**, does not necessarily lead to a particular high antiproliferative activity. In fact, the increased electrostatic interactions brought by the positively charged nitrogens largely decrease the cytotoxic activity in all cell lines tested. Again, the binding of the polyamines chain which profoundly affect the DNA structure (e.g., aggregation and condensation) might explain the unexpected low antiproliferative activity of **16**.[30]

Compound **14** was next selected for in vivo antitumor evaluation. Tumors were inoculated by subcutaneous injection of BT474 breast cancer cells in the mammary gland of immunosupressed mice (NOG/SCID). The compound was administrated ip, at 20 and 60 mg/kg, dissolved in 0.9% NaCl. Control mice received an equivalent volume of vehicle alone, following an identical schedule. At day 44 of treatment, tumor volume was increased by 732.9 $\pm$ 475.2% in control mice, as compared to 499.5 $\pm$ 141.7% and 195.47 $\pm$ 114.6% in mice treated with 20 and 60 mg/kg of compound **14**, representing an $\sim$32 and 73% reduction of tumor volume, respectively, showing an in vivo antitumor effect of this compound.

Caspases Activation. To gain more mechanistic insights into the antiproliferative activity of the compounds, caspase-3/7 activity was next determined in SKBR3 breast cancer cells as it is a downstream executioner of caspases, responsible for physiological and morphological changes that occur in apoptosis.[36] Therefore, it was interesting to evaluate the effect of our compounds on the activity of caspase-3/7 and to compare the results with their parent ammonium. As shown in Figure 4, the antiproliferative activity of guanidinium **8** and **14** correlated with high caspase-3/7 activation. It is important to notice that none of the amines tested were found to activate caspase-3/7. Interestingly, guanidine **6** and amine **13** appeared to display moderate antiproliferative activity in the absence of significant caspase-3/7 activation suggesting that their antiproliferative activity involved caspase-3/7-independent mechanisms. Moreover, all the other compounds, which bear either a guanidine (**2** and **16**) or an amine (**1**, **5**, and **7**) function, were found to have no effect whatsoever. Hence, the guanidinium group appears to be essential, yet not sufficient, for caspase-3/7 activation.

Intracellular Distribution. To obtain a more precise insight into the possible mechanism of its antiproliferative effect, the intrinsic fluorescence properties of the pyrene ring in **14** were exploited to assess the cellular uptake and the intracellular distribution of the drug. Figure 5 shows fluorescent images of SKBR3 breast cancer cells exposed to **14**. To target mitonchondria functions, the cells were treated with Mito Tracker for 45 min at 37 °C, followed by 10 μM of **14** for 1 h at 37 °C; they were then washed and fixed using CytoFix buffer. **14** was detected under ultraviolet (480 nm) excitation. Figure 5 clearly shows that **14** essentially accumulates within the cell nuclei (blue staining) but also partly colocalizes with mitochondria labeling (violet staining), indicating that the cytotoxic action of **14** is likely driven by the drug binding to nucleic acids and possibly also mitochondria functional alterations. These results are particularly important since it is well-documented that drugs bearing the guanidino group usually influence the mitochodrial functions located in the cytoplasm.[20,21,37]

Conclusion

Several different polyaromatic guanidinium derivatives were synthesized, and their DNA-binding properties and antiproliferative activities against various tumor cell lines were compared with those of the corresponding ammonium precursors. Viscometric titration indicated that these compounds lengthen the DNA helix as much as the analogous monfunctional intercalator ethidium bromide. As expected, guanidinium derivatives interacted more strongly with DNA. In the case of the human SKBR3 breast carcinoma cells, we were able to find, for a given structure, a correlation between DNA affinity and cytotoxicity, guanidinium derivatives being more potent than their ammonium counterparts. Compound **14**, which possesses a broad spectrum of antitumoral activity, was found to accumulate preferentially in the cell nuclei. As such, it represents the first guanidino intercalator that penetrates into the cell and exhibits selective nuclear uptake capacity. These compounds are capable of forming stronger DNA complexes than their amino parents, which is in accordance with their in vitro activities and was further confirmed by in vivo experiments. These results suggest that the electronic nature of the chain tethering an intercalator not only influences the DNA-binding process but might be used to tune the new DNA−drug complex toward increasing the cytotoxicities of drugs. As this work provides new evidence that small structural alterations result in substantial differences in biological activities, it raises new opportunities for the development of innovative intercalative drugs and offers a rational basis for better understanding the structural requirements of molecules that interact with nuclear DNA. In view of the high importance of amino derivatives in cancer therapies (e.g.,

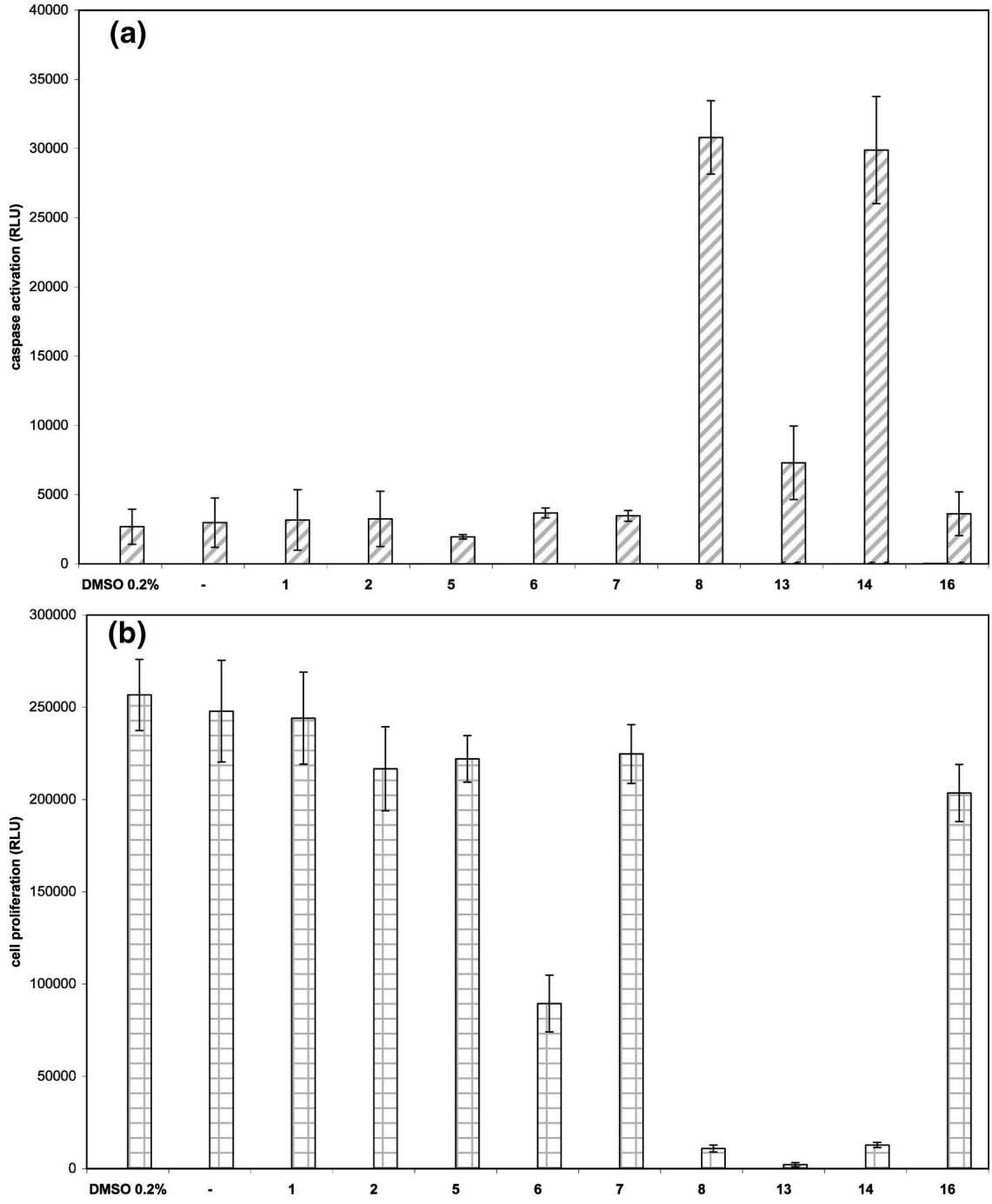

Figure 4. (a) Drug-induced activation of caspase-3/7 in SKBR3 cells. Cells were exposed to various compounds (20 μM). (b) SKBR3 cell proliferation in the presence of 20 μM of the same compounds. Control experiments were run in the presence and absence (-) of DMSO 0.2%.

doxorubicin, daunomycin etc.), this study sheds new light on the development of more active drugs.

Experimental Section

Melting points were determined with a Stuart Scientific melting point apparatus SM3 and are uncorrected. Most compounds darkened when heated and decomposed (dec) at the melting point. ^{1}H and ^{13}C NMR spectra were recorded employing a Bruker DRX spectrometer. The chemical shifts are expressed in parts per million relative to the residual proton signals in deuteriosolvents as internal standards when deuteriochloroform or deuteriomethanol were used. High resolution mass spectra were recoded on a JEOL SV102 using 3-nitrobenzyl alcohol or a mixture of glycerol and thioglycerol as a matrix when the fast atom bombardment (FAB) method was employed or on a Q-TOF Micromass when the electrospray inonization (ESI) method was employed. All chemical reagents and solvents were purchased from commercial sources and used without further purification. Ethidium bromide and amines **1**, **3**, and **9** were purchased from Aldrich. Hoechst 33258 was purchased from Acros. The synthesis of intermediates **20**−**21**,[24] guanidinium **2**,[38] and amines **7**[39] and **11**[40,41] have been previously reported. Calf thymus DNA (CT-DNA) was purchased from Calbiochem and used without further purification. The stock solutions of CT-DNA were prepared by dissolving CT-DNA in sodium cacodylate−HCl buffer (10 mM sodium cacodylate, pH 7.0) or BPE buffer (6 mM Na_2HPO_4, 2 mM NaH_2PO_4, 1 mM EDTA, pH 7.0) and sonicated for 20 cycles, where each cycle consisted of 30 s of sonication with 30 s intervals. A solution of CT-DNA prepared as mentioned above in both buffer gave a ratio of UV absorbance at 260 and 280 nm of more than 1.8, indicating that the DNA was sufficiently free from protein.

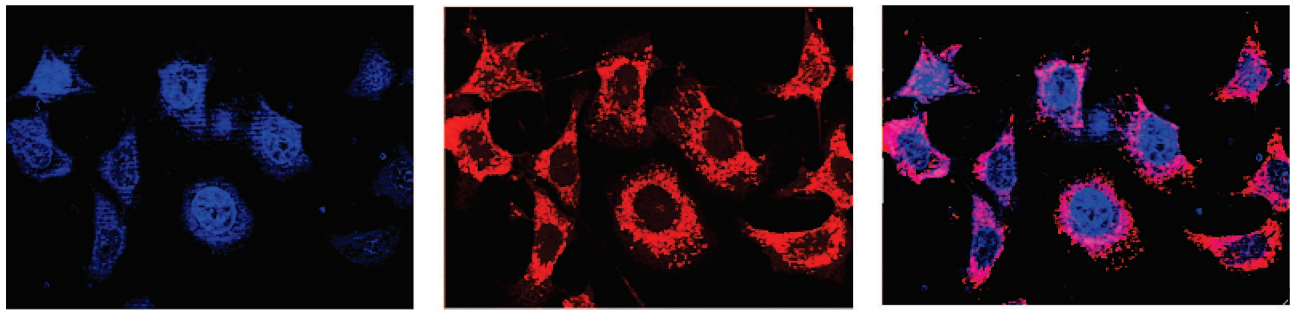

Figure 5. Fluorescence microscopy of SKBR3 cells treated with Mito Tracker for 45 min (red fluorescence) followed by **14** at 10 μM for 1 h (blue fluorescence). The right panel image corresponds to superimposed red and blue fluorescences.

The concentration of the CT-DNA expressed in terms of base pairs was determined by UV absorbance measurements using the molar absorption coefficient (12 824 M^{-1} cm^{-1}) at 260 nm. The stock solutions were stored at 4 °C and used no more than 4 days after preparation. Synthetic 12mer oligodeoxynucleotides were purchased from Eurogentec and used as received. These were stored as concentrated stock solutions in water at −20 °C. The concentrations of these oligodeoxynucleotides expressed in terms of strands were determined by UV absorbance measurements using the molar extinction coefficient 138 500 M^{-1} cm^{-1} for d(AGAATTGGGTGT) and 124 700 M^{-1} cm^{-1} for d(ACACCCAATTCT) at 260 nm.

General Procedure for Reductive Amination. To a stirred solution of the amine (0.25 M) in MeOH/THF (1/1) was added the aldehyde (1 equiv). The mixture was stirred at room temperature overnight until the imine formation was complete (monitored by TLC). The reaction mixture was then cooled to 0 °C and $NaBH_4$ (3 equiv) was added in small portions. After stirring for 1 h at 0 °C, the solution was further stirred for 45 min at room temperature. The reaction mixture was diluted with AcOEt and water. The organic layer was separated, washed with brine, dried over anhydrous $MgSO_4$, filtered, and concentrated under vacuum. The residue was purified by silica gel chromatography.

General Procedures for the Synthesis of Guanidines. To a mixture of the amine in dry DMF (1 M) was added 1*H*-pyrazole-1-carboxamidine hydrochloride (1 equiv) and diisopropylethylamine (DIEA) (1 equiv). The reaction mixture was stirred at room temperature under an argon atmosphere. After stirring overnight, the solvent was removed under vacuum and the crude product was recrystallized to give the pure guanidines.

General Procedure for HCl Salt Formation. Gaseous HCl was bubbled into a solution of the respective amine, Boc-protected amine, or bis-Boc-protected guanidine in MeOH (0.11 M). After stirring for 1 h, the solvent was removed under vacuum. To the resultant residue was added MeOH and Et_2O, and the resulting precipitate was collected, washed, and dried.

2-Thiophenemethylguanidine Hydrochloride (4). 4 was obtained from 2-thiophenemethylamine following the general procedure for guanidylation. Recrystallization from EtOH and Et_2O gave **4**. Light yellow solid (yield 29%); mp 122–123 °C; ^{1}H NMR (300 MHz, CD_3OD) δ 4.61 (s, 2H), 7.01 (dd, 1H, J = 3.5, 5.0), 7.10 (d, 1H, J = 3.0), 7.39 (dd, 1H, J = 0.9, 5.0); ^{13}C NMR (75 MHz CD_3OD) δ 40.96, 126.87, 127.61, 128.08, 140.09, 158.45; HRMS (FAB) found 156.0593 $[M + H]^+$ calcd for $C_6H_{10}N_3S$ 156.0595.

2-Fluorenemethylamine Hydrochloride (5). To a stirred solution of 2-fluorenecarboxaldehyde (2.91 g, 15.00 mmol) and hydroxylamine hydrochloride (2.08 g, 29.98 mmol) in EtOH (36 mL) and H_2O (12 mL) was added sodium acetate trihydrate (6.12 g, 44.97 mmol). The solution was heated at 70 °C for 30 min. After the mixture was cooled, the solvent was removed in vacuo and the resultant solid was dissolved in water and extracted with ether. The organic layer was washed with brine, dried over $MgSO_4$, and then concentrated under vacuum. Recrystallization of the residue from AcOEt and Hexane gave fluorene-2-carboxaldehyde oxime (1.81 g, 8.63 mmol, 58% as a mixture of syn/anti isomer) as a colorless crystalline solid. mp 158–159 °C; ^{1}H NMR (300 MHz $CDCl_3$, peaks of major isomer were described) δ 3.92 (s,2H), 6.6–7.2 (br s, 1H), 7.29–7.84 (m, 7H), 8.24 (s, 1H); ^{13}C NMR (75 MHz $CDCl_3$) δ 36.96, 120.25, 120.45, 123.51, 125.29, 126.57, 127.09, 127.54, 130.34, 141.07, 143.86, 143.89, 143.93, 150.96; HRMS (FAB) found 210.0921 $[M + H]^+$ calcd for $C_{14}H_{12}NO$ 210.0919, also found 209.0847 $[M]^{\bullet+}$ calcd for $C_{14}H_{11}NO$ 209.0841.

A suspension of the previously prepared oxime (1.04 g, 5.00 mmol) and 5% Pd/C (523 mg) in MeOH (15 mL) and AcOEt (15 mL) was stirred under a hydrogen atmosphere for 2 h. After filtration over celite, the mixture was concentrated under vacuum. The residue was purified by silica gel chromatography ($Et_3N/CHCl_3$: 5/95) to give the free amine (596 mg, 61%) as a white solid. **5** was obtained quantitatively from the free amine following the general procedure for HCl salt formation. White solid; mp > 248 °C (dec); ^{1}H NMR (300 MHz CD_3OD) δ 3.94 (s, 2H), 4.19 (s, 2H), 7.26–7.69 (m, 5H), 7.79–7.93 (m, 2H); ^{13}C NMR (75 MHz CD_3OD) δ 37.58, 44.63, 121.19, 121.38, 126.19, 126.82, 128.04, 128.47, 128.85, 132.69, 142.00, 144.04, 144.82, 145.54; HRMS (FAB) found 196.1106 $[M + H]^+$ calcd for $C_{14}H_{14}N$ 196.1126.

2-Fluorenemethylguanidine Hydrochloride (6). 6 was obtained from **5** following the general procedure for guanidylation. Recrystallization from MeOH and $CHCl_3$ gave **6**. White solid (yield 23%); mp 205–206 °C; ^{1}H NMR (300 MHz CD_3OD) δ 3.90 (s, 2H), 4.47 (s, 2H), 7.23–7.40 (m, 3H), 7.50–7.59 (m, 2H), 7.76–7.87 (m, 2H); ^{13}C NMR (75 MHz CD_3OD) δ 37.58, 46.26, 120.93, 121.12, 125.21, 126.10, 127.25, 127.93, 128.07, 136.05, 142.32, 142.95, 144.66, 145.32, 158.67; HRMS (FAB) $[M + H]^+$ found 238.1349 calcd for $C_{15}H_{16}N_3$ 238.1344.

9-Anthracenemethyl Azide (17). To a suspension of 9-anthracenemethanol[22] (1.54 g, 7.39 mmol) in CH_2Cl_2 (30 mL) was added dropwise at 0 °C $SOCl_2$ (810 μL, 11.10 mmol). The mixture was then allowed to react for 1 h at 0 °C. The solvent was removed in vacuo, and the resultant residue was precipitated with 10 mL of a 1:1 solution of Et_2O and hexane. After filtration, the precipitate was dissolved in DMF (20 mL), and sodium azide (777 mg, 11.95 mmol) was added in one portion. The reaction mixture was heated for 1 h at 50 °C, cooled to room temperature, and diluted with 50 mL of water. After extraction with AcOEt, the organic layer was washed with brine, dried over $MgSO_4$ and concentrated under vacuum. Purification of the residue by silica gel chromatography (AcOEt/hexane 5/95) gave **17** (1.369 g, 79% from 9-anthracenemethanol). Yellow solid; mp 84–86 °C; ^{1}H NMR (300 MHz $CDCl_3$) δ 5.34 (s, 2H), 7.52 (t, 2H, J = 7.5 Hz), 7.56–7.64 (m, 2H), 8.06 (d, 2H, J = 8.3 Hz), 8.30 (d, 2H, J = 8.9 Hz), 8.52 (s, 1H); ^{13}C NMR (75 MHz $CDCl_3$) δ 46.50, 123.66, 125.36, 125.93, 127.00, 129.15, 129.45, 130.86, 131.53; HRMS (FAB) found 233.0944 $[M]^{\bullet+}$ calcd for $C_{15}H_{11}N_3$ 233.0953.

9-Anthracenemethylguanidine Hydrochloride (8). 8 was obtained from 9-anthracencemethylamine following the general procedure for guanidylation. Recrystallization from MeOH and Et_2O gave **8**. Yellow solid (yield 73%); mp 266–267 °C; ^{1}H NMR (300 MHz CD_3OD) δ 5.36 (s, 2H), 7.54 (t, 2H, J = 7.5), 7.59–7.69 (m, 2H), 8.12 (d, 2H, J = 8.4 Hz), 8.27 (d, 2H, J = 8.9 Hz), 8.62 (s, 1H); ^{13}C NMR (75 MHz CD_3OD) δ 39.15, 124.28, 126.40, 126.65, 128.25, 130.15, 130.49, 131.75, 133.03, 158.58; HRMS (FAB) found 250.1351 $[M+H]^+$ calcd for $C_{16}H_{16}N_3$ 250.1344.

1-Pyrenemethylguanidine Hydrochloride (10). 10 was obtained from pyrenemethylamine following the general procedure for guanidylation. Recrystallization from MeOH and Et_2O gave **10**. Brown solid (yield 56%); mp 271–272 °C; ^{1}H NMR (300 MHz CD_3OD) δ 5.14 (s, 2H), 8.00–8.31 (m, 9H); ^{13}C NMR (75 MHz CD_3OD) δ 44.67, 123.27, 125.72, 126.00, 126.16, 126.64, 126.78, 127.27, 127.45, 128.38, 128.87, 129.53, 130.01, 130.09, 132.09, 132.68, 132.69, 158.69; HRMS (FAB) found 274.1341 $[M + H]^+$ calcd for $C_{18}H_{16}N_3$ 274.1344.

[4-[(Pyrene-1-ylmethyl)amino]butyl]carbamic Acid *tert*-Butyl Ester (19). 19 was obtained from (4-amino-butyl)-carbamic acid *tert*-butyl ester[41] following the general procedure for reductive amination. White solid (yield 59%): mp 105–108 °C; R_f = 0.27 (AcOEt/hexane/Et_3N: 50/50/5); ^{1}H NMR (300 MHz $CDCl_3$) δ 1.43 (s, 9H), 1.46–1.70 (m, 4H), 2.43 (br s, 1H), 2.82 (t, 2H, J = 6.7 Hz), 3.12 (br dd, 2H), 4.49 (s, 2H), 4.76 (br s, 1H), 7.95–8.06 (m, 4H), 8.10–8.24 (m, 4H), 8.35 (d, 1H, J = 9.2 Hz); ^{13}C NMR (75 MHz $CDCl_3$) δ 27.20, 27.99, 28.57, 40.52, 49.38, 51.59, 79.21, 123.18, 124.86, 125.00, 125.16, 125.21, 125.30, 126.06, 127.32, 127.58, 127.94, 129.26, 130.94, 130.96, 131.44, 133.08, 156.18; HRMS (FAB) found 403.2393 $[M + H]^+$ calcd for $C_{26}H_{31}N_2O_2$ 403.2386.

***N*^{1}-(Pyrene-1-ylmethyl)-1,4-diaminobutane Dihydrochloride (13). 13** was obtained from **19** following the general procedure for HCl salt formation. Light yellow solid (yield 84%); mp > 246 °C (dec); ^{1}H NMR (300 MHz D_2O) δ 1.44–1.67 (m, 4H), 2.85 (t, 2H, J = 7.2 Hz), 2.95 (t, 2H, J = 7.5 Hz), 4.30 (s, 2H), 7.35–7.99 (m, 9H); ^{13}C NMR (75 MHz D_2O) δ 22.65, 23.91, 38.68, 46.47, 47.74, 120.87, 122.49, 122.90, 123.09, 124.44, 125.53, 125.63, 126.24, 126.80, 127.82, 128.09, 128.31, 129.61, 130.34, 131.29; HRMS (FAB) found 303.1871 $[M + H]^+$ calcd for $C_{21}H_{23}N_2$ 303.1861.

***N*^{2},*N*^{3}-Bis(*tert*-butoxycarbonyl)-*N*^{1}-[4-[(anthracene-9-ylmethyl) amino]butyl] Guanidine (23). 23** was obtained from 1-amino-4-[N^2,N^3-bis(*tert*-butoxycarbonyl)-guanidino]butane **20**[24] following the general procedure for reductive amination. Brown oil (yield 62%); R_f = 0.45 (AcOEt/hexane/Et_3N: 30/70/5); ^{1}H NMR (300 MHz, $CDCl_3$) δ 1.47 (s, 9H), 1.51 (s, 9H), 1.56–1.73 (m, 4H), 2.87 (t, 2H, J = 6.7 Hz), 3.38 (br dd, 2H), 4.79 (s, 2H), 7.40–7.51 (m, 2H), 7.51–7.60 (m, 2H), 8.00 (d, 2H, J = 8.4 Hz), 8.34 (d overlapped by br s, 3H), 8.42 (s, 1H), 11.5 (br s, 1H); ^{13}C NMR (75 MHz, $CDCl_3$) δ 26.88, 27.10, 28.19, 28.46, 40.64, 45.37, 49.51, 79.53, 83.21, 124.16, 125.14, 126.50, 127.74, 129.32, 130.57, 131.63, 153.41, 156.34, 163.72; HRMS (FAB) found 521.3138, $[M + H]^+$ calcd for $C_{30}H_{41}N_4O_4$ 521.3128.

[4-[(Anthracene-9-ylmethyl)-amino]butyl] guanidine Dihydrochloride (12). 12 was obtained quantitatively from **23** following the general procedure for HCl salt formation. Yellow solid; mp > 236 °C (dec); ^{1}H NMR (300 MHz D_2O) δ 1.31–1.66 (m, 4H), 2.86–3.09 (m, 4H), 7.42 (t, 2H, J = 7.5 Hz), 7.47–7.57 (m, 2H), 7.87 (m, 4H), 8.23 (s, 1H); ^{13}C NMR (75 MHz, D_2O) δ 22.68, 25.06, 40.31, 42.35, 47.03, 120.33, 122.34, 125.42, 127.61, 129.39, 130.01, 130.29, 130.62, 156.59; HRMS (FAB) found 321.2098 $[M + H]^+$ calcd for $C_{20}H_{25}N_4$ 321.2079.

***N*^{2},*N*^{3}-Bis(*tert*-butoxycarbonyl)-*N*^{1}-[4-[(pyrene-1-ylmethyl) amino]butyl] Guanidine (24). 24** was obtained from 1-amino-4-[N^2,N^3-bis(*tert*-butoxycarbonyl)-guanidino]butane **20**[24] following the general procedure for reductive amination. Light yellow solid (yield 75%); mp > 121 °C (dec); R_f = 0.33 (AcOEt/hexane/Et_3N: 40/60/5); ^{1}HMR (300 MHz $CDCl_3$) δ 1.47 (s, 9H), 1.50 (s, 9H), 1.57–1.70 (m, 4H), 2.21 (br s, 1H), 2.82 (br t, 2H), 3.43 (br dd, 2H), 4.50 (s, 2H), 7.95–8.23 (m, 8H), 8.31–8.43 (m, 2H), 11.51 (br s, 1H); ^{13}C NMR (75 MHz $CDCl_3$) δ 27.03, 27.24, 28.18, 28.45, 40.79, 49.36, 51.68, 79.42, 83.18, 123.22, 124.84, 125.00, 125.16, 125.24, 126.01, 127.23, 127.24, 127.58, 127.86, 129.24, 130.86, 130.96, 131.43, 133.42, 153.43, 156.31, 163.75; HRMS (FAB) found 545.3137 $[M + H]^+$ calcd for $C_{32}H_{41}N_4O_4$ 545.3128.

[4-[(Pyrene-1-ylmethyl)amino]butyl] Guanidine Dihydrochloride (14). 14 was obtained from **24** following the general procedure for HCl salt formation. Recrystallization of the precipitate from MeOH and Et_2O gave **14**. Light yellow solid (yield 81%); mp 248–249 °C; ^{1}H NMR (300 MHz D_2O) δ 1.19–1.35 (m, 2H), 1.35–1.52 (m, 2H), 2.74–2.91 (m, 4H), 4.29 (s, 2H), 7.37–7.98 (m, 9H); ^{13}C NMR (75 MHz, D_2O) δ 22.64, 24.87, 40.21, 46.34, 47.47, 120.88, 122.52, 122.98, 123.16, 124.49, 125.56, 125.68, 126.27, 126.84, 127.88, 128.15, 128.41, 129.66, 130.38, 131.34, 156.44; HRMS (FAB) found 345.2053 $[M + H]^+$ calcd for $C_{22}H_{25}N_4$ 345.2079.

***N*^{2},*N*^{3}-Bis(*tert*-butoxycarbonyl)-*N*^{1}-[6-[(pyrene-1-ylmethyl)-amino]hexyl] Guanidine (25). 25** was obtained from 1-amino-6-[N^2,N^3-bis(*tert*-butoxycarbonyl)-guanidino]hexane **21**[24] following the general procedure for reductive amination. Yellow solid (yield 40%); mp > 100 °C (dec); R_f = 0.38 (AcOEt/hexane/Et_3N: 40/60/5); ^{1}H NMR (300 MHz $CDCl_3$) δ 1.30–1.40 (m, 4H), 1.48 (s, 9H), 1.50 (s, 9H), 1.53–1.67 (m, 4H), 2.77 (t, 2H, J = 7.2 Hz), 3.38 (dd, 2H, J = 7.0, 12.4 Hz), 4.48 (s, 2H), 7.94–8.05 (m, 4H), 8.10–8.22 (m, 4H), 8.29 (br t, 1H), 8.35 (d, 1H, J = 9.3 Hz), 11.5 (s, 1H); ^{13}C NMR (75 MHz $CDCl_3$) δ 26.85, 27.11, 28.20, 28.45, 29.06, 29.80, 40.00, 49.75, 51.63, 79.34, 83.12, 123.20, 124.84, 125.00, 125.16, 125.23, 126.01, 127.24, 127.26, 127.57, 127.87, 129.22, 130.86, 130.95, 131.42, 133.33, 153.45, 156.23, 163.79; HRMS (FAB) found 573.3431 $[M + H]^+$ calcd for $C_{34}H_{45}N_4O_4$ 573.3441.

[6-[(Pyrene-1-ylmethyl)amino]hexyl] Guanidine Dihydrochloride (15). 15 was obtained from **25** following the general procedure for HCl salt formation. The resulted residue was washed with Et_2O and lyophilized to give **15**. Light brown solid (yield 80%); ^{1}H NMR (300 MHz CD_3OD) δ 1.35–1.55 (m, 4H), 1.62 (qu, 2H, J = 6.8 Hz), 1.74–1.91 (m, 2H), 3.18 (t, 2H, J = 7.0 Hz), 3.22–3.29 (m, 2H), 5.00 (s, 2H), 8.03–8.25 (m, 4H), 8.26–8.38 (m, 4H), 8.46 (d, 1H, J = 9.3 Hz); ^{13}C NMR (75 MHz CD_3OD) δ 27.05, 27.16, 27.27, 29.61, 49.08, 49.37, 123.19, 125.56, 125.59, 126.05, 126.15, 126.99, 127.22, 127.71, 128.31, 129.74, 129.89, 130.17, 131.10, 131.99, 132.64, 133.88, 158.63; HRMS (FAB) found 373.2402 $[M + H]^+$ calcd for $C_{24}H_{29}N_4$ 373.2392.

***N*^{2},*N*^{3}-Bis(*tert*-butoxycarbonyl)-*N*^{1}-[3-[[4-[(3-aminopropyl)-amino]butyl]amino]propyl] guanidine (22).** To a solution of spermine (343 mg, 1.70 mmol) in DMF (15 mL) was added dropwise a solution of *N*,*N*′-bis-Boc-thiourea (235 mg, 0.85 mmol) in DMF (10 mL). The reaction mixtire was stirred for 1.5 h and diluted with $CHCl_3$ (20 mL) and brine (20 mL). The organic layer was separated, dried over Na_2SO_4, and concentrated under vacuum. Purification of the resulting residue by silica gel chromatography (Et_3N/MeOH 5/95) gave **22**. Colorless oil (yield 52%); ^{1}H NMR (300 MHz $CDCl_3$) δ 1.31–1.55 (m, 22H), 1.55–1.77 (m, 4H), 2.48–2.69 (m, 8H), 2.74 (t, 2H, J = 6.7 Hz), 3.44 (t, 2H, J = 6.6 Hz), 8.45 (br s, 1H); ^{13}C NMR (75 MHz $CDCl_3$) δ 27.61, 27.67, 28.12, 28.36, 29.23, 32.79, 38.99, 40.54, 46.98, 47.81, 49.65, 79.26, 83.07, 153.19, 156.32, 163.57; HRMS (FAB) found 445.3481 $[M + H]^+$ calcd for $C_{21}H_{45}O_4N_6$ 445.3502.

***N*^{2},*N*^{3}-Bis(*tert*-butoxycarbonyl)-*N*^{1}-[3-[[4-[[3-[(pyrene-1-ylmethyl)-*tert*-butoxycarbonylamino]propyl]-*tert*-butoxycarbonylamino]butyl]-*tert*-butoxycarbonylamino]propyl] guanidine (27).** To a solution of compound **22** (140 mg, 0.32 mmol) in MeOH (0.6 mL) and THF (0.6 mL) was added 1-pyrenecarboxaldehyde (74 mg, 0.32 mmol) in one portion. The reaction mixture was allowed to react for 14 h and was then cooled to 0 °C with an ice bath. After addition of $NaBH_4$ (34 mg, 0.90 mmol) at 0 °C, the ice bath was removed and the reaction was stirred for 4 h. The mixture was then diluted with water and AcOEt. The organic layer was washed with brine, dried over Na_2SO_4, and then concentrated in vacuo. Purification of the residue by silica gel chromatography (MeOH/CH_2Cl_2/Et_3N 10/90/5) gave a crude triamine compound **26**, which was used immediately without further purification. To a solution of crude **26** in CH_2Cl_2 (2.0 mL) was added a solution of Boc_2O (124 mg, 0.57 mmol) in CH_2Cl_2 (3.0 mL). The mixture was stirred for 12 h and then diluted with water and Et_2O. The organic layer was washed with brine, dried over Na_2SO_4, and then concentrated in vacuo. Purification of the residue by silica gel chromatography (AcOEt/hexane 25/75) gave **27**. Colorless oil (yield 26% from **22**); ^{1}H NMR (300 MHz $CDCl_3$) δ 0.95–1.65 (br m, 51H), 1.65–1.85 (br m, 2H), 2.55–3.54 (br m, 12H), 5.20 (s, 2H), 7.80–8.57 (m, 10H), 11.49 (br s, 1H); ^{13}C NMR (75 MHz $CDCl_3$)

δ 25.53, 25.82, 27.36, 28.15, 28.40, 28.49, 28.55, 28.65, 38.74, 44.17, 44.71, 46.39, 46.74, 47.01, 48.47, 79.26, 79.53, 80.06, 83.33, 124.79, 124.86, 125.10, 125.31, 126.13, 127.45, 127.50, 127.96, 130.89, 131.40, 153.24, 155.43, 155.73, 156.15, 163.15; HRMS (ESI) found 959.5841 $[M + H]^+$ calcd for $C_{53}H_{79}N_6O_{10}$ 959.5858.

[3-[[4-[[3-[(1-Pyrenemethyl)amino]propyl]amino]butyl]amino]propyl] Guanidine Tetrahydrochloride (16). Compound **27** (83 mg, 0.09 mmol) was stirred in HCl−MeOH (10 M, 7 mL) at room temperature. After 3 h, the solvent was removed in vacuo to give **16**. Yellow solid (yield 84%); mp 237–240 °C; ^{1}H NMR (300 MHz D_2O) δ 1.45–1.72 (m, 4H), 1.74–2.09 (m, 4H), 2.80–3.04 (m, 8H), 3.06–3.26 (m, 4H), 4.67 (s, 2H), 7.71–8.24 (m, 9H); ^{13}C NMR (75 MHz D_2O) δ 22.69, 24.94, 38.13, 44.20, 44.48, 44.85, 46.85, 46.88, 48.23, 121.44, 123.15, 123.34, 123.69, 124.87, 125.85, 126.02, 126.64, 127.14, 128.30, 128.62, 128.90, 129.95, 130.66, 131.79, 156.78; HRMS (FAB) found 459.3231 $[M + H]^+$ calcd for $C_{28}H_{39}N_6$ 459.3236.

Absorption Spectrophotometry and Melting Temperature Studies. Absorption spectra and melting curves were measured using a Varian Cary 300 BIO UV–visible spectrophotometer equipped with a thermoelectric temperature controller. Titrations of the drug with DNA were performed by adding aliquots of a concentrated DNA solution to a drug solution at constant ligand concentration. The solutions were equilibrated for 5 min at 25 °C after each addition, and the absorption spectra were recorded in the range 500–200 nm (in the case of titration of EtBr, the range is 700–200 nm) until no further decrease in absorbance was observed. The binding affinities were calculated using absorbance spectra according to the McGhee and Von Hippel equation using data point from Scatchard plots.[29] The binding data were fitted using Kaleidagraph 4.0 software.

For each series of T_m measurements, samples were placed in a thermostatically controlled cell holder and the quartz cuvettes (10 mm path length) were heated by circulating water with a heating rate of 0.5 °C/min. The measurements with CT-DNA (4 μM bp) were performed in BPE buffer, pH 7.0 (6 mM Na_2HPO_4, 2 mM NaH_2PO_4, 1 mM EDTA) in the absence or presence of the drug (2 μM) over the range 20–100 °C. The measurements with d(ACACCCAATTCT) and its complementary strand d(AGAATTGGGTGT) (2 μM each) were performed in sodium cacodylate buffer (9.8 mM, pH 7.0) in the absence or presence of the drug (12 μM) over the range 0–95 °C. The melting temperature T_m was determined from the first derivatives of the melting curve obtained.

Viscometric Titrations. Sonicated calf thymus DNA (42% GC, Calbiochem) was prepared in 5 mM Tris/Tris-H^+, EDTA (0.5 mM) buffer (pH 7.0), and 10% DMSO. The average molecular weight of the fragments produced after sonication was determined to be 1.6×10^6 Da by viscometric analysis.[33] The flow times (t_b) of buffer without (t_o) and with DNA (t; 0.8 mM bp) were used to calculate the intrinsic viscosity in the presence or absence of the drugs. The relative lengthening of the helix L/L_0 is proportional to the intrinsic viscosity, resulting in the following equation: $L/L_0 = (\eta/\eta_0)^{1/3}$. Guanidines were added as stock solutions in buffer/DMSO to give a final binding ratio of 0.12. Viscosity measurements were made with a Schott Micro-Ubbelohde viscometer with a capillary diameter of 0.53 mm. The viscometer was submerged in a water bath to maintain a constant temperature of 23.00 ± 0.1 °C. All measurements were averaged over three trials to an accuracy of ±0.2 s. The value of L/L_0 was plotted for each experiment as a function of r. Slopes were generated by conducting linear least-squared fits to these data. Ethidium bromide and Hoechst 33258 were run as controls for these experiments.

In Vitro Screening. T47D (human breast carcinoma, ATCC HTB-133), SKBR3 (human breast carcinoma, ATCC HTB-30), and HT29 (human colon carcinoma, ATCC HTB-38) were cultivated in Dulbecco's MEM supplemented with 10% calf serum (FCS) and 1 mM pyruvate. BT474 (human breast carcinoma, ATCC HTB-20) was cultivated in RPMI supplemented with 10% FCS, 1% insuline/Transferrin/selenium-X (GIBCO). PC-3 (human prostate carcinoma, ATCC CRL-1435) and LnCAP (human prostate carcinoma, ATCC CRL-1740) were cultivated in RPMI supplemented with 10% FCS.

Exponentially growing cell cultures were seeded in 96-well plates (5000 cells/100 μL culture medium per well) and incubated for 24 h, followed by addition of increasing concentrations of the tested compounds in DMSO solution, in triplicate. Corresponding volumes of DMSO were distributed as control. Plates were reincubated for 72 h before evaluation of the cell survival using the CellTiter 96 aqueous one solution cell proliferation assay (Promega) as recommended by the manufacturer. Briefly, 20 μL of CellTiter solution was added to the wells, followed by 3 h of incubation at 37 °C and measurement of absorbance at 540 nm using a MultiScan EX (Labsystems) microplate reader. The ratio cytostatic/cytotoxic was calculated as triplicate mean values deduced from blank control values and expressed as IC_{50}, the concentration that reduced by 50% the number of treated cells relative to controls. IC_{50} values were extracted from regression curves obtained with experimental points.

In Vivo Experiment. The in vivo effects of **14** were preliminarily explored in nonobese diabetic gamma C−/− severe combined immunodeficiency mice (NOG/SCIDγc^{null}) using established subcutaneously flank-implanted BT474 cells. After counting, 5×10^6 cells were resuspended in 400 μL Matrigel (Becton Dickinson, France) and immediately injected subcutaneously to allow solidification. Following 10–15 days after injection, mice with established xenografts received 3 day interval intraperitoneal injections, with 100 μL 0.9% NaCl or **14** formulated in 0.9% NaCl. Tumour volumes were calculated from direct tumor measurements using a caliper and with the formula volume = 0.52(length × width^2). Each group was formed of five animals. All mice were kept at the CRCM animal facilities, and all experiments were performed in accordance with institutional guidelines.

Caspase-3/7 Activity. Caspase-3/7 activities were determined in homogeneous cell lysates using the Caspase-Glo 3/7 assay, as recommended by the manufacturer (Promega, France). Briefly, 10^4 cells per 45 μL were seeded in 96-well plates followed by the addition of 5 μL of tested compounds for 24 h of incubation. After incubation, 50 μL Caspase-Glo 3/7 assay were added and luciferase activity was measured using a luminometer (Centro, Berthold, France).

Confocal Microscopy. The SKBR3 cells were seeded in 24-well plates, on coverslips (50 000 cells/500 μL culture medium per well) and incubated for 24 h. Mito Tracker (Molecular Probes) was used as recommended by the manufacturer. Briefly, 100 nM Mito Tracker was added to cell cultures for 45 min at 37 °C followed by 10 μM of **14**, for 1 h at 37 °C. Corresponding volumes of DMSO were distributed as control. The medium was removed, and cells were rinsed with ice-cold PBS followed by fixation in CytoFix for 20 min at 4 °C (BD Pharmingen) as recommended by the manufacturer. Following washing ice-cold PBS, antifade solution was used to mount the stained coverslips. The fluorescence signals were detected using an Apo Tome workstation (Zeiss) with a 63 × 1.4 NA oil objective, equipped with an HBO 100 W lamp, with excitation at 365 using a 395 dichroic mirror followed by a 445/50 filter set for detection of **14**, or with excitation at 546/12 using a 560 dichroic mirror followed by a 575/640 filter set for detection of Mito Tracker. Operating conditions were set up so that detectable images could not be obtained for control cell samples.

Acknowledgment. We gratefully acknowledge financial support from Université de Montpellier 2 and the Regional Council Provence Alpes Cotes d'Azur. The authors thank Daniel Isnardon for his contributions to the fluorescence microscopy analyses and Dr Olivia Gianni for her help with the viscometric titrations. A.R. was a fellow of an ANRS grant. We thank the reviewers for their helpful comments.

Supporting Information Available: Purity data from HPLC analysis and ^{1}H NMR and ^{13}C NMR spectra of all new target

compounds. This material is available free of charge via the Internet at http://pubs.acs.org.

References

(1) Dervan, P. B. Molecular recognition of DNA by small molecules. *Bioorg. Med. Chem.* **2001**, *9*, 2215–2235.
(2) Demeunynck, M.; Bailly, C.; Wilson, W. D. *DNA and RNA Binders*; Wiley-VCH: Weinheim, 2002.
(3) Lerman, L. S. Structural Considerations in Interaction of DNA and Acridines. *J. Mol. Biol.* **1961**, *3*, 18–30.
(4) Lerman, L. S. Structure of DNA-Acridine Complex. *Proc. Natl. Acad. Sci. USA* **1963**, *49*, 94–102.
(5) Brana, M. F.; Cacho, M.; Gradillas, A.; de Pascual-Teresa, B.; Ramos, A. Intercalators as anticancer drugs. *Curr. Pharm. Des.* **2001**, *7*, 1745–1780.
(6) Martinez, R.; Chacon-Garcia, L. The search of DNA-interealators as antitumoral drugs: What it worked and what did not work. *Curr. Med. Chem.* **2005**, *12*, 127–151.
(7) Malonne, H.; Atassi, G. DNA topoisomerase targeting drugs: mechanisms of action and perspectives. *Anti-Cancer Drugs* **1997**, *8*, 811–822.
(8) Banik, B. K.; Becker, F. F. Polycyclic aromatic compounds as anticancer agents: Structure-activity relationships of chrysene and pyrene derivatives. *Bioorg. Med. Chem.* **2001**, *9*, 593–605.
(9) Wunz, T. P.; Craven, M. T.; Karol, M. D.; Hill, G. C.; Remers, W. A. DNA-Binding by Antitumor Anthracene-Derivatives. *J. Med. Chem.* **1990**, *33*, 1549–1553.
(10) Iyengar, B. S.; Dorr, R. T.; Alberts, D. S.; Solyom, A. M.; Krutzsch, M.; Remers, W. A. 1,4-disubstituted anthracene antitumor agents. *J. Med. Chem.* **1997**, *40*, 3734–3738.
(11) Dorr, R. T.; Liddil, J. D.; Sami, S. M.; Remers, W.; Hersh, E. M.; Alberts, D. S. Preclinical antitumor activity of the azonafide series of anthracene-based DNA intercalators. *Anti-Cancer Drugs* **2001**, *12*, 213–220.
(12) Rescifina, A.; Chiacchio, M. A.; Corsaro, A.; De Clercq, E.; Iannazzo, D.; Mastino, A.; Piperno, A.; Romeo, G.; Romeo, R.; Valveri, V. Synthesis and biological activity of isoxazolidinyl polycyclic aromatic hydrocarbons: Potential DNA intercalators. *J. Med. Chem.* **2006**, *49*, 709–715.
(13) Kamal, A.; Ramesh, G.; Srinivas, O.; Ramulu, P. Synthesis and antitumour activity of pyrene-linked pyrrolo [2,1-c][1,4]benzodiazepine hybrids. *Bioorg. Med. Chem. Lett.* **2004**, *14*, 471–474.
(14) Banik, B. K.; Becker, F. F. Synthesis, electrophilic substitution and structure-activity relationship studies of polycyclic aromatic compounds towards the development of anticancer agents. *Curr. Med. Chem.* **2001**, *8*, 1513–1533.
(15) Bair, K. W.; Tuttle, R. L.; Knick, V. C.; Cory, M.; McKee, D. D. (1-Pyrenylmethyl)Amino Alcohols, a New Class of Antitumor DNA Intercalators - Discovery and Initial Amine Side-Chain Structure Activity Studies. *J. Med. Chem.* **1990**, *33*, 2385–2393.
(16) Bair, K. W.; Andrews, C. W.; Tuttle, R. L.; Knick, V. C.; Cory, M.; McKee, D. D. 2-[(Arylmethyl)Amino]-2-Methyl-1,3-Propanediol DNA Intercalators—An Examination of the Effects of Aromatic Ring Variation on Antitumor-Activity and DNA-Binding. *J. Med. Chem.* **1991**, *34*, 1983–1990.
(17) Ohara, K.; Smietana, M.; Vasseur, J. J. Characterization of specific noncovalent complexes between guanidinium derivatives and single-stranded DNA by MALDI. *J. Am. Soc. Mass Spectrom.* **2006**, *17*, 283–291.
(18) Stephens, C. E.; Tanious, F.; Kim, S.; Wilson, W. D.; Schell, W. A.; Perfect, J. R.; Franzblau, S. G.; Boykin, D. W. Diguanidino and "reversed" diamidino 2,3-diarylfurans as antimicrobial agents. *J. Med. Chem.* **2001**, *44*, 1741–1748.
(19) Dardonville, C.; Barrett, M. P.; Brun, R.; Kaiser, M.; Tanious, F.; Wilson, W. D. DNA binding affinity of bisguanidine and bis(2-aminoimidazoline) derivatives with in vivo antitrypanosomal activity. *J. Med. Chem.* **2006**, *49*, 3748–3752.
(20) Andreani, A.; Granaiola, M.; Leoni, A.; Locatelli, A.; Morigi, R.; Rambaldi, M.; Lenaz, G.; Fato, R.; Bergamini, C.; Farruggia, G. Potential antitumor agents. 37. Synthesis and antitumor activity of guanylhydrazones from imidazo[2,1-b]thiazoles and from the new heterocyclic system thiazolo[2′,3′: 2,3]imidazo [4,5-c]quinoline. *J. Med. Chem.* **2005**, *48*, 3085–3089.
(21) Ekelund, S.; Nygren, P.; Larsson, R. Guanidino-containing drugs in cancer chemotherapy: biochemical and clinical pharmacology. *Biochem. Pharmacol.* **2001**, *61*, 1183–1193.
(22) Ostaszewski, R.; Wilczynska, E.; Wolszczak, M. The synthesis of a new type of anthracene DNA intercalator. *Bioorg. Med. Chem. Lett.* **1998**, *8*, 2995–2996.
(23) Bernatowicz, M. S.; Wu, Y. L.; Matsueda, G. R. 1-*H*-Pyrazole-1-Carboxamidine Hydrochloride—An Attractive Reagent for Guanylation of Amines and Its Application to Peptide-Synthesis. *J. Org. Chem.* **1992**, *57*, 2497–2502.
(24) Carmignani, M.; Volpe, A. R.; Botta, B.; Espinal, R.; De Bonnevaux, S. C.; De Luca, C.; Botta, M.; Corelli, F.; Tafi, A.; Sacco, R.; Delle Monache, G. Novel hypotensive agents from Verbesina caracasana. 8. Synthesis and pharmacology of (3,4-dimethoxycinnamoyl)-N-1-agmatine and synthetic analogues. *J. Med. Chem.* **2001**, *44*, 2950–2958.
(25) Modukuru, N. K.; Snow, K. J.; Perrin, B. S.; Bhambhani, A.; Duff, M.; Kumar, C. V. Tuning the DNA binding modes of an anthracene derivative with salt. *J. Photochem. Photobiol. A: Chem.* **2006**, *177*, 43–54.
(26) Becker, H. C.; Norden, B. DNA binding thermodynamics and sequence specificity of chiral piperazinecarbonyloxyalkyl derivatives of anthracene and pyrene. *J. Am. Chem. Soc.* **2000**, *122*, 8344–8349.
(27) Becker, H. C.; Norden, B. DNA binding mode and sequence specificity of piperazinylcarbonyloxyethyl derivatives of anthracene and pyrene. *J. Am. Chem. Soc.* **1999**, *121*, 11947–11952.
(28) Oliveira, M.; Baptista, A. L. F.; Coutinho, P. J. G.; Castanheira, E. M. S.; Hungerford, G. Fluorescence studies of the interaction of pyrenylmethyl tributylphosphonium bromide with double-strand polynucleotides. *Photochem. Photobiol. Sci.* **2004**, *3*, 217–225.
(29) McGhee, J. D.; Von Hippel, P. H. Theoretical Aspects of DNA-Protein Interactions - Cooperative and Non-Cooperative Binding of Large Ligands to a One-Dimensional Homogeneous Lattice. *J. Mol. Biol.* **1974**, *86*, 469–489.
(30) Bloomfield, V. A. DNA condensation. *Curr. Opin. Struct. Biol.* **1996**, *6*, 334–341.
(31) Geall, A. J.; Taylor, R. J.; Earll, M. E.; Eaton, M. A. W.; Blagbrough, I. S. Synthesis of cholesteryl polyamine carbamates: pK(a) studies and condensation of calf thymus DNA. *Bioconjugate Chem.* **2000**, *11*, 314–326.
(32) Suh, D.; Chaires, J. B. Criteria for the Mode of Binding of DNA-Binding Agents. *Bioorg. Med. Chem.* **1995**, *3*, 723–728.
(33) Cohen, G.; Eisenberg, H. Viscosity and Sedimentation Study of Sonicated DNA-Proflavine Complexes. *Biopolymers* **1969**, *8*, 45–55.
(34) Dedon, P. C. Determination of Binding Mode: Intercalation. *Curr. Protoc. Nucleic Acid Chem.* **2000**, 8.1.18.1.13.
(35) Bailly, C.; Arafa, R. K.; Tanious, F. A.; Laine, W.; Tardy, C.; Lansiaux, A.; Colson, P.; Boykin, D. W.; Wilson, W. D. Molecular determinants for DNA minor groove recognition: Design of a bis-guanidinium derivative of ethidium that is highly selective for AT-rich DNA sequences. *Biochemistry* **2005**, *44*, 1941–1952.
(36) Denault, J. B.; Salvesen, G. S. Caspases: Keys in the ignition of cell death. *Chem. Rev.* **2002**, *102*, 4489–4499.
(37) Andreani, A.; Burnelli, S.; Granaiola, M.; Leoni, A.; Locatelli, A.; Morigi, R.; Rambaldi, M.; Varoli, L.; Farruggia, G.; Stefanelli, C.; Masotti, L.; Kunkel, M. W. Synthesis and antitumor activity of guanylhydrazones from 6-(2,4-dichloro-5-nitrophenyl)imidazo[2,1-b]thiazoles and 6-pyridylimidazo[2,1-b]thiazoles. *J. Med. Chem.* **2006**, *49*, 7897–7901.
(38) Dijols, S.; Boucher, J. L.; Lepoivre, M.; Lefevre-Groboillot, D.; Moreau, M.; Frapart, Y.; Rekka, E.; Meade, A. L.; Stuehr, D. J.; Mansuy, D. First non-alpha-amino acid guanidines acting as efficient NO precursors upon oxidation by NO-Synthase II or activated mouse macrophages. *Biochemistry* **2002**, *41*, 9286–9292.
(39) Kumar, C. V.; Asuncion, E. H. DNA-Binding Studies and Site-Selective Fluorescence Sensitization of an Anthryl Probe. *J. Am. Chem. Soc.* **1993**, *115*, 8547–8553.
(40) Wang, C. J.; Delcros, J. G.; Cannon, L.; Konate, F.; Carias, H.; Biggerstaff, J.; Gardner, R. A.; Phanstiel, O. Defining the molecular requirements for the selective delivery of polyamine conjugates into cells containing active polyamine transporters. *J. Med. Chem.* **2003**, *46*, 5129–5138.
(41) Gardner, R. A.; Delcros, J. G.; Konate, F.; Breitbeil, F.; Martin, B.; Sigman, M.; Huang, M.; Phanstiel, O. *N*-1-Substituent effects in the selective delivery of polyamine conjugates into cells containing active polyamine transporters. *J. Med. Chem.* **2004**, *47*, 6055–6069.

JM701207M